

DRIFTS and Knudsen cell study of the heterogeneous reactivity of SO₂ and NO₂ on mineral dust

M. Ullerstam¹, M. S. Johnson², R. Vogt³, and E. Ljungström¹

¹Gothenburg University, Department of Chemistry, SE-41296 Gothenburg, Sweden

²Copenhagen University, Department of Chemistry, Universitetsparken 5, DK-2100 Copenhagen, Denmark

³Ford Forschungszentrum GmbH Aachen, Süsterfeldstrasse 200, D-52072 Aachen, Germany

Received: 14 July 2003 – Published in Atmos. Chem. Phys. Discuss.: 28 July 2003

Revised: 10 November 2003 – Accepted: 12 November 2003 – Published: 25 November 2003

Abstract. The heterogeneous oxidation of SO₂ by NO₂ on mineral dust was studied using Diffuse Reflectance Infrared Fourier Transform Spectroscopy (DRIFTS) and a Knudsen cell. This made it possible to characterise, kinetically, both the formation of sulfate and nitrate as surface products and the gas phase loss of the reactive species. The gas phase loss rate was determined to be first order in both SO₂ and NO₂. From the DRIFTS experiment the uptake coefficient, γ , for the formation of sulfate was determined to be of the order of 10^{-10} using the BET area as the reactive surface area. No significant formation of sulfate was seen in the absence of NO₂. The Knudsen cell study gave uptake coefficients of the order of 10^{-6} and 10^{-7} for SO₂ and NO₂ respectively. There was no significant difference in uptake when SO₂ or NO₂ were introduced individually compared to experiments in which SO₂ and NO₂ were present at the same time.

1 Introduction

Particulate matter present in the Earth's atmosphere provides reactive surfaces for heterogeneous chemistry. A large contribution to the tropospheric aerosol budget is mineral aerosol that originates from arid and semi-arid areas. The annual flux of mineral aerosol to the atmosphere is estimated to be between 1000 and 3000 Tg, and with changes in precipitation patterns and land use, the emissions of mineral aerosol may increase substantially which would increase their importance in the atmosphere (Dentener, et al., 1996; Tegen and Fung, 1994; Zhang and Carmichael, 1999). Atmospheric aerosol particles are known to affect radiative transfer by scattering and absorbing light and they can also influence the optical properties of clouds. Understanding interactions between the gas and the condensed phase is important because these pro-

cesses may influence the photochemical oxidation capacity of the atmosphere as well as changing aerosol composition and size distribution (Dentener et al., 1996; Galy-Lacaux et al., 2001; Martin et al., 2003; Zhang and Carmichael, 1999). Recent modeling work has shown how aerosols modify the chemical properties of the atmosphere, decreasing the photolysis rate of ozone and the concentration of HO_x, increasing the concentration of CO, and producing HNO₃ from NO₂ and NO₃ (Martin et al., 2003).

Field measurements of the chemical composition of aerosol particles in East Asia show strong correlations between nitrate and non-sea-salt calcium (i.e. the mineral aerosol fraction) (Carmichael et al., 1996; Nishikawa et al., 1991; Zhang et al., 2000). Such a correlation, while not as strong, is also seen for non-sea-salt sulfate and mineral aerosol (Carmichael et al., 1996; Nishikawa et al., 1991; Zhang et al., 2000). The observed correlations could be caused by surface reactions of sulfur and nitrogen species. An indication that particles originating from soil are more likely to contain a mixture of sulfate and nitrate than other kinds of particles has also been found (Zhang et al., 2000).

However, large uncertainties remain concerning the effect of chemical composition and surface properties on heterogeneous reaction kinetics.

In the present study, the heterogeneous reaction of SO₂ and NO₂ on mineral dust was investigated using the Knudsen cell and Diffuse Reflectance Infrared Fourier Transform Spectroscopy (DRIFTS) techniques. Mineral dust samples from the Cape Verde Islands, located off Mauritania and Senegal on the west coast of Africa, were used for the experiments. The mineral dust consists of a <20 μm diameter fraction and has a BET surface area of $5 \times 10^5 \text{ cm}^2 \text{ g}^{-1}$. The samples are representative of mineral dust from the Saharan desert and the main content of the samples is quartz and potassium feldspars (Desboeufs et al., 1999; Rognon et al., 1996).

Correspondence to: M. Ullerstam
(mullerst@chem.utoronto.ca)

Table 1. Knudsen Reactor Parameters.

Knudsen reactor parameter	
reactor volume, V	$3,72 \pm 0.03 \text{ dm}^3$
experimental temperature, T_{exp}	$299 \pm 0.2 \text{ K}$
geometric sample area, A_{geo}	33.2 cm^2
escape orifice (pulsed flow), ϕ	11 mm
escape rate (calculated), k_{esc}	1.00 s^{-1}
escape rate (measured), k_{esc}	$(1.10 \pm 0.20) \text{ s}^{-1}$
escape orifice (steady state flow), ϕ	2 mm
escape rate (calculated), k_{esc}	0.067 s^{-1}

2 Experimental

2.1 Knudsen cell experiments

A Knudsen cell was used for the analysis of loss from the gas phase due to surface reactions or adsorption. The Knudsen cell reactor consists of a chamber with an isolated sample compartment and a small orifice through which gas phase reactant and product species can escape to be detected by mass spectrometry. To assure molecular flow, the mean free path must be at least a factor of 10 greater than the diameter of the exit orifice, which was maintained by a low pressure in the cell (Golden et al., 1973). The Knudsen reactor setup has previously been described (Mønster et al., 2002). The reaction chamber is a 6-way ISO 100 cross sealed with Viton O-rings, which is connected to a quadrupole mass spectrometer (Leda Mass). Inside the reactor a plunger makes it possible to either cover or expose the sample holder. To minimize wall reactions the reactor walls were passivated with a coating of Teflon. The temperature of the sample holder can be controlled from 233 to 373 K using a Peltier cooler and a cryofluid pump. The design of the gas system makes it possible to introduce the reactive gases in two ways, either through a pulsed valve or as a continuous flow through needle valves. The pulsed valve is a solenoid valve (General Valve P/N 009-1562-900) with a 0.8 millimetre orifice, and can generate pulses from a few hundred microseconds to several hours at a repetition rate of up to 2500 Hz. The use of a pulsed valve in combination with a Knudsen cell was first described by Tabor et al. (1994). The system uses a dual needle valve (Nupro) to regulate the gas flow in the steady state mode.

The dust samples were applied to the sample holder using an atomizer containing a water suspension of the mineral dust. The aerosol is sprayed onto the sample holder which was preheated to 373 K. This procedure enables the formation of a thin uniform surface of the mineral dust. The sample was kept in the evacuated reaction chamber at 333 K for 1 h prior to experiments. This treatment has been shown to give a reproducible reactivity, and removes loosely bound water from the sample (Ullerstam et al., 2002). After the system

was cooled to room temperature the plunger was lowered and the sample was covered. A fresh mixture of the reactive gases with known concentration was made before every experiment and was introduced into the chamber either as a pulse or as a steady state flow. Parameters for the Knudsen reaction chamber can be found in Table 1.

NO_2 (>98%, Hede Nielsen) and SO_2 (99.9%, Gerling Holtz and Company) were used for the Knudsen cell experiments.

2.2 Experiments using the DRIFTS technique

The DRIFTS technique was used to analyse the surface reactions. Infrared spectra were recorded in the spectral range from 4000 to 600 cm^{-1} with a Bruker Equinox 55 FTIR spectrometer equipped with a mercury cadmium telluride (MCT) detector and DRIFTS optics (model DRA-2CO, Harrick Scientific Corp.). General features of the setup have previously been described (Borensen et al., 2000; Ullerstam et al., 2002). Spectra were recorded at a resolution of 4 cm^{-1} and 100 scans were averaged for each spectrum resulting in a time resolution of 1 min. The dust samples were prepared as a water suspension on glass plates, with dimensions of $9 \times 9 \text{ mm}^2$ followed by drying in an oven (10 min, 333 K). The reaction chamber was flushed with He carrier gas while the sample was kept at 333 K for 1 h at a pressure of 4.5 mbar before an experiment was started. Spectra were collected as difference spectra with the unreacted dust as the background, thus surface products appear as positive bands while losses of surface species give rise to negative bands. Surface reactants were quantified by ion chromatography using a Dionex DX 120 system, equipped with a Dionex AS 14 analytical column and a conductivity detector (CD 20) with detection stabilizer. A more detailed description of the analysis is available (Ullerstam, et al., 2002).

NO_2 for the DRIFTS experiments was synthesized from the reaction between NO (>99.5%, Messer-Griesheim) and O_2 (>99.998%, Messer-Griesheim). SO_2 (>99.98%, Messer-Griesheim) was diluted with He before use.

3 Results

3.1 Observed products

The unexposed dust sample is used to collect a background spectrum and therefore both positive and negative features were observed in the subsequent spectra. Investigations were made in which mineral dust was reacted just with NO_2 , or with SO_2 and NO_2 simultaneously using the DRIFTS technique. When only NO_2 was added a number of absorption bands were observed, as can be seen in Fig. 1a. The most prominent positive features are two bands between 1500 and 1300 cm^{-1} which can be assigned to the degenerate asymmetric stretch vibration of the nitrate ion (Borensen et al.,

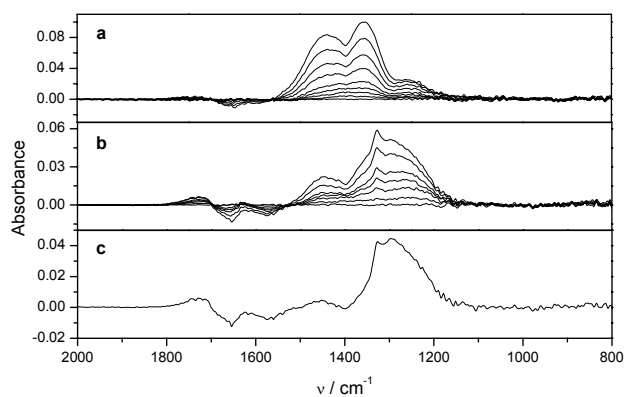


Fig. 1. Absorption difference spectra recorded during the reaction of mineral dust with SO_2 and NO_2 . (a) experiment where the surface is exposed to NO_2 only ($[\text{NO}_2]=2.2 \times 10^{13}$ molecule cm^{-3}) after a reaction time of 5, 10, 20, 30 and 50 min. (b) experiment with exposure of both SO_2 and NO_2 ($[\text{SO}_2]=9.4 \times 10^{12}$ and $[\text{NO}_2]=2.5 \times 10^{13}$ in molecule cm^{-3}) after a reaction time of 2, 5, 10, 15, 30 and 50 min. (c) residue from subtraction of final spectrum of NO_2 experiment in (a) from the final spectrum of SO_2/NO_2 experiment in (b).

2000; Hadjiivanov et al., 1994; Nakamoto, 1997; Underwood et al., 1999). The splitting of the ν_3 vibration is due to an interaction with the surface, resulting in a reduced symmetry for the nitrate species. The nitrate ion can coordinate to a metal as a unidentate, chelating bidentate or bridging bidentate ligand. It is difficult to distinguish between these possibilities since the symmetry differs very little (Nakamoto, 1997). At lower wavenumbers at the end of the nitrate band at 1250 cm^{-1} there is a smaller positive band that may be assigned to the asymmetric stretch of nitrite (Borensen et al., 2000; Hadjiivanov et al., 1994). Both nitrate and nitrite ions are found in the ion chromatography analysis. A small negative band is also present at 1650 cm^{-1} indicating loss of surface species originating from surface-adsorbed water (Nakamoto, 1997). This loss of water during the reaction is also seen as a negative band in the area around 3200 cm^{-1} . The loss of different types of free OH groups at the surface is evidenced as a small negative band at 3700 cm^{-1} (not shown in figure) (Tsyganenko and Mardilovich, 1996). When SO_2 is introduced simultaneously with NO_2 the bands of nitrate are still dominant, especially when the ratio of SO_2 to NO_2 is low, cf. Fig. 1b. However at higher ratios the bands of sulfur species become evident. The small narrow band at 1330 cm^{-1} on the top of the broader nitrate band is due to physisorbed SO_2 (Chang, 1978; Datta et al., 1985; Deo and Dalla Lana, 1971; Goodman et al., 2001; Nakamoto, 1997; Ullerstam et al., 2002). The nitrate band is also to some extent distorted and the nitrite band is superimposed on the band of surface bound sulfate at 1240 cm^{-1} (Meyer et al., 1980; Schoonheydt and Lunsford, 1972; Ullerstam et al., 2002; Usher et al., 2002). There are indications that the

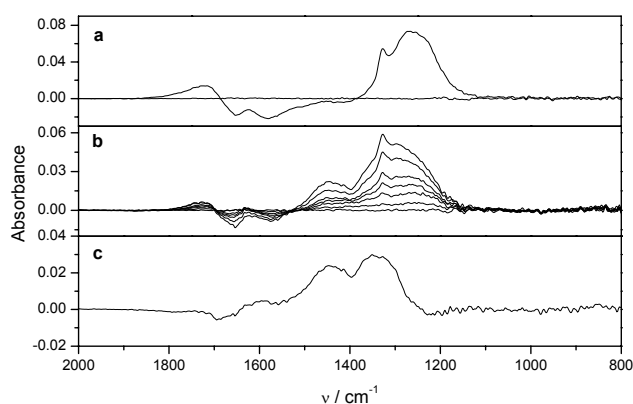


Fig. 2. Absorption difference spectra recorded during the reaction of mineral dust with SO_2 and NO_2 . (a) reference spectrum of sulfur species from reaction of SO_2 on mineral dust in the presence of O_3 (Ullerstam et al., 2002). (b) experiment with exposure of both SO_2 and NO_2 ($[\text{SO}_2]=9.4 \times 10^{12}$ and $[\text{NO}_2]=2.5 \times 10^{13}$ in molecule cm^{-3}) after a reaction time of 2, 5, 10, 15, 30 and 50 min. (c) residue from subtraction of reference spectrum (a) from the final spectrum of SO_2/NO_2 experiment in (b).

formation of nitrite on the surface is inhibited by the introduction of SO_2 over the surface. The loss of free OH groups is larger when SO_2 is present which indicates that SO_2 is adsorbed to these free OH groups while NO_2 may adsorb on other reactive sites as well. A broad band at 2450 cm^{-1} during exposure to SO_2 also indicates some formation of hydrogen sulfite (Meyer et al., 1980; Nakamoto, 1997). Subtraction of the nitrate features in the spectra derived from experiments with both SO_2 and NO_2 present, using the pure NO_2 experiment as a reference, results in a spectrum with a band around 1280 cm^{-1} (Fig. 1c) which is assigned to the sulfate band although shifted 40 cm^{-1} relative to the band of surface bound sulfate. The peak at 1330 cm^{-1} is due to physisorbed SO_2 which is not subtracted. A similar procedure was made to subtract the sulfate band revealing the nitrate features between 1500 and 1300 cm^{-1} which can be seen in Fig. 2c. It should be noted that spectra shown in Figs. 1b and 2b are identical spectra from the same experiment. The reference spectra (a) in Fig. 2 with features of physisorbed SO_2 and SO_4^{2-} were obtained from an earlier experiment with the same substrate (Ullerstam et al., 2002). Weak features below 1000 cm^{-1} may not be detectable due to the low signal-to-noise ratio in this region.

3.2 Kinetics, Knudsen cell

The total uptake coefficient (γ_{total}) is defined as the fraction of collisions with the surface that results in loss of the molecule from the gas phase divided by the total number of surface collisions per unit time. From the Knudsen experiments this can be calculated from the first order rate

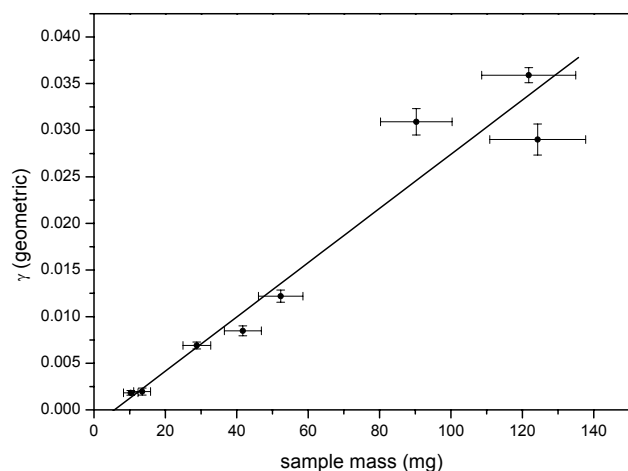


Fig. 3. Total uptake coefficient for SO₂ calculated using the geometric surface area as the effective surface area as a function of sample mass. Experiments were performed with a pulsed flow of a mixture of SO₂ and NO₂ (2.7×10^{11} and 1.7×10^{11} molecules, respectively).

coefficient of the uptake (k_f), the collision frequency (Z) and the reactive surface area (A_s).

$$\gamma_{\text{total}} = \frac{k_f}{Z \times A_s} \quad (1)$$

$$Z = \sqrt{\frac{8 \times R \times T}{\pi \times M}} \times \frac{1}{4V} \quad (2)$$

where R is the gas constant ($\text{J mol}^{-1} \text{K}^{-1}$), T is the temperature (K) and V is the volume of the reactor (m^3).

The data treatment of the first order rate coefficient (k_f) depends on whether the reactive gases are introduced as a pulse or as a steady state flow. In an experiment with pulsed flow the decay rate is measured with and without the sample covered. The decay is equal to the lifetime of the gas in the chamber which is the inverse of the loss rate, $k=1/\tau$. Experiments are performed with the sample holder covered or open.

$$k_{Kc} = k_e \quad (3)$$

$$k_{Kc+s} = k_e + k_u \quad (4)$$

Here “Kc” signifies Knudsen cell; “e”, escape; “u”, uptake and “s”, sample exposed. Rearranging gives,

$$k_u = k_{Kc+s} - k_{Kc} \quad (5)$$

Thus k_u in Eq. (5) is equal to the first order rate coefficient (k_f) in Eq. (1) and no knowledge of the theoretical value of k_e is necessary. The value k_e is the theoretical escape rate coefficient for the specific gas and aperture.

$$k_e = Z \times A_h \quad (6)$$

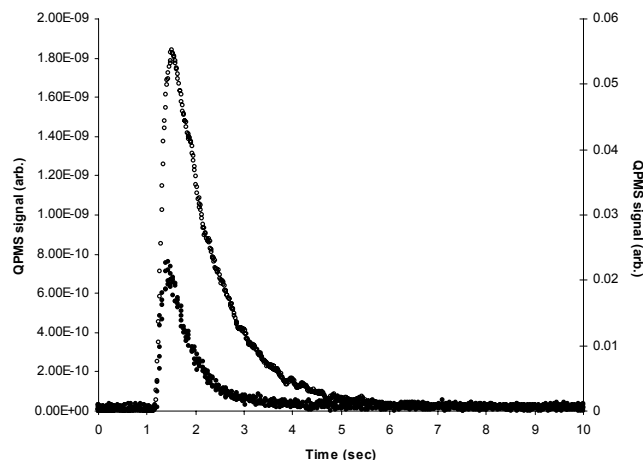


Fig. 4. An example of a typical Knudsen experiment performed with a pulsed flow showing the decay of the SO₂ signal ($m/z=64$). Initial concentrations of SO₂ and NO₂ were 2.7×10^{11} and 1.7×10^{11} in molecules cm^{-3} , respectively. Empty circles represent the decay of SO₂ signal when the surface is covered, see right y-axis. Filled circles represent the decay of SO₂ signal during exposure of the sample surface, see left y-axis.

where A_h is the area of the escape aperture, corrected for the limitation to the flow caused by the nonzero length of the aperture.

For a steady state flow experiment, the first order rate coefficient is obtained by measuring the relative intensity of the signal before (S_0) and during (S_R) the exposure of the sample according to Eq. (7).

$$k_f = k_e \left(\frac{S_0}{S_R} - 1 \right) \quad (7)$$

The initial drop in the signal is used to obtain S_R .

To study the dependence of the uptake coefficient on sample mass, using the geometric area (projected surface) as the effective surface area, a number of experiments with different sample mass but constant concentration of SO₂ and NO₂ were performed; the results are shown in Fig. 3. This was done to ensure that experiments were conducted in the linear mass regime where the entire sample participates in the reaction and the BET surface area can be used as the reactive surface area (Grassian, 2002; Underwood et al., 2000). These experiments were made with a pulsed flow where each pulse contained a mixture of SO₂ and NO₂ (2.7×10^{11} and 1.7×10^{11} molecules, respectively). An example of a typical experiment is shown in Fig. 4. The resulting uptake coefficient for SO₂ was determined to be $(1.6 \pm 0.1) \times 10^{-5}$ using the BET area as the reactive surface area.

A number of experiments were carried out using a constant concentration of NO₂ while the concentration of SO₂ was varied, to study the uptake coefficient of SO₂ in the presence of NO₂. Another set of experiments was made with different concentrations of NO₂ but constant concentration of

Table 2. Reactive uptake coefficients and other experimental data for the reaction of SO₂ and NO₂ with mineral dust at 299 K. BET surface area, 5.0×10⁵ (cm² g⁻¹).

[SO ₂] molecule cm ⁻³	[NO ₂] molecule cm ⁻³	γ(SO ₂) geometric	γ(SO ₂) BET	γ(NO ₂) geometric	γ(NO ₂) BET
(2.6–87)×10 ¹¹	9.8×10 ¹²	^a (1.5±0.6)×10 ⁻³	^a (5.7±1.9)×10 ⁻⁶	–	–
(5.4–15)×10 ¹²	–	^a (1.3±0.3)×10 ⁻³	^a (4.6±0.3)×10 ⁻⁶	–	–
5.3×10 ¹²	(1.7–10)×10 ¹²	–	–	^a (2.0±0.4)×10 ⁻⁴	^a (6.3±1.0)×10 ⁻⁷
–	(1.0–1.5)×10 ¹³	–	–	^a (1.9±0.4)×10 ⁻⁴	^a (6.2±3.4)×10 ⁻⁷
(1.4–9.3)×10 ¹²	2.4×10 ¹³	^b (1.6±0.6)×10 ⁻⁶	^b (2.6±1.1)×10 ⁻¹⁰		

^aKnudsen experiment^bDRIFTS experiments

SO₂ to obtain the uptake coefficient of NO₂ in the presence of SO₂. A typical experiment is shown in Fig. 5. All the experiments were made with a steady state flow of the reactive gases and the sample mass was kept at around 20 mg of mineral dust to maintain “linear mass” conditions. A summary of the results can be found in Table 2. The errors are reported at the 95% confidence interval, as determined from the standard deviation of an ensemble of experiments. It can be seen that the results from the steady state experiment give an uptake coefficient that is around 3 times smaller relative to the pulsed experiments. The discrepancy may be caused by the lower time resolution of a steady state experiment. In a steady state experiment, the true initial uptake coefficient may be hidden because of the time required to lift the sample cover (Mønster et al., 2002). It can also be seen from Fig. 5 that there is a time dependence of the uptake coefficient which indicates surface saturation. This could be due to either the consumption of reactive sites on the surface by an irreversible uptake mechanism or by the equilibrium of a reversible process. At the end of the experiment the signal has not been recovered and is still growing but very slowly. Some part of the discrepancy is also due to a base-line drift during the experiment.

The observed relative loss of SO₂ and NO₂ from the gas phase during the experiments was 63±10 and 18±5% respectively. A log-log plot of the initial loss rate of SO₂ versus the concentration of SO₂ shown in Fig. 6, gives a slope of 1.02±0.24 (2σ) i.e. the SO₂ loss has an apparent first order dependence on [SO₂]. An equivalent plot was made for NO₂ which gave a slope of 0.86±0.18 (2σ) which also indicates a reaction order of 1 for NO₂ which is shown in Fig. 7. This means that in both cases the adsorption rate depends on the concentration of the reactive species and that the uptake coefficient is independent of concentration.

3.3 Kinetics, DRIFTS

The amount of sulfate on the sample was determined by ion chromatography in order to quantify the sulfate forma-

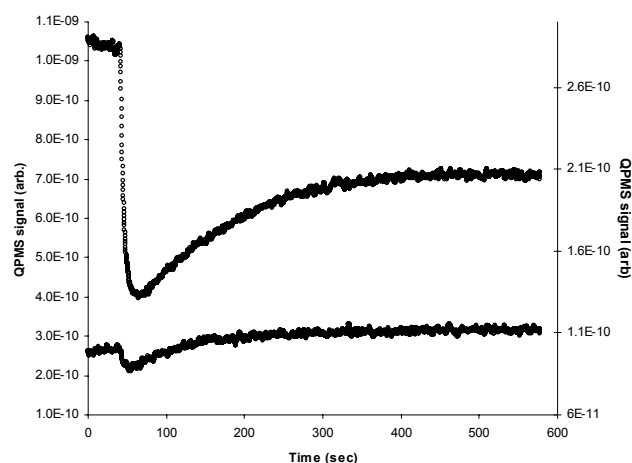


Fig. 5. An example of a typical Knudsen experiment performed with a steady state flow. Steady state concentrations of SO₂ and NO₂ were 5.0×10¹² and 1.0×10¹³ molecules cm⁻³, respectively. The top line represents the signal for SO₂ (m/z=64) and belong to the left y-axis. The lower line represents the signal for NO₂ (m/z=46) and belong to the right y-axis.

tion rate $d[\text{SO}_4^{2-}]/dt$ in terms of the reactive uptake coefficient. The initial formation rate was translated from absorption units s⁻¹ to SO₄²⁻ s⁻¹ by a conversion factor obtained from a calibration plot. The calibration plot is obtained from the ion chromatography analysis where the entire sample is used for the analysis assuming that the reaction products are evenly distributed in the sample. Since the absorption bands of the different reaction product species overlap one another, the bands are deconvoluted before integration. The reactive uptake coefficient (γ_{rxn}) is defined as the rate of sulfate formation on the surface ($d[\text{SO}_4^{2-}]/dt$) divided by the total number of surface collisions per unit time (Ω).

$$\gamma_{rxn} = \frac{d[\text{SO}_4^{2-}]/dt}{\Omega} \quad (8)$$

$$\Omega = \frac{1}{4} \times A_s \times [\text{SO}_2] \times v_{\text{SO}_2} \quad (9)$$

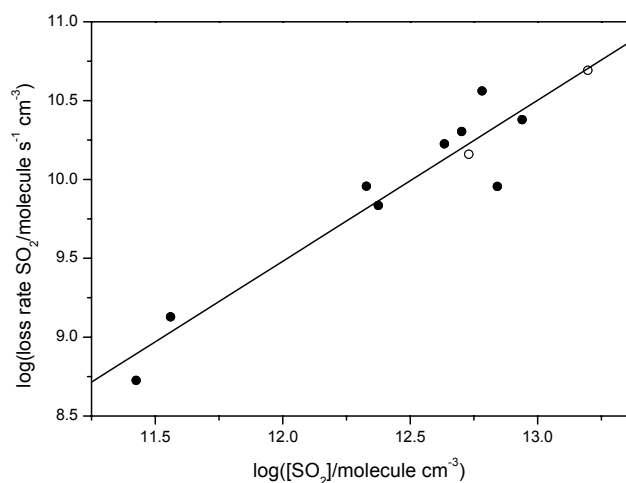


Fig. 6. A bilogarithmic plot of the loss rate of SO_2 as a function of $[\text{SO}_2]$. Filled circles are experiments with SO_2 and NO_2 present, open circles are from experiments with only SO_2 present. From linear regression of experiments with both SO_2 and NO_2 present (filled circles) the reaction order was determined to be $n=1.01\pm 0.15$ (2σ), $r^2=0.98$.

where v is the mean molecular velocity of SO_2 calculated as $\sqrt{8RT/\pi M_{\text{SO}_2}}$ and A_s is the effective sample surface. $d[\text{SO}_4^{2-}]/dt$ was obtained from the absorbance/time plot at t_0 i.e. the initial rate, thus no saturation effects on γ are expected.

A sequence of experiments was performed with a constant concentration of NO_2 and varying concentrations of SO_2 . The results can be seen in Table 2. The observed relative loss from the gas phase resulting in reactive species on the surface was between 1.5% to 7.8% and 0.15% to 0.57% for SO_2 and NO_2 respectively. The experiments that were terminated at a short reaction time were the ones with largest relative loss from the gas phase. This is expected since the loss rate of reactive species is fast in the initial phase of the experiment but decreases with increasing exposure due to the loss of reactive sites on the surface.

The introduction of SO_2 to the reactive gas reduces the formation of surface nitrate species compared to experiment with only NO_2 . From the ion chromatography analysis at the end of the experiment in which only NO_2 was introduced, the total amount of surface nitrate was 2.1×10^{16} ions ($[\text{NO}_2]=2.2 \times 10^{13}$ molecule cm^{-3} , reaction time=160 min). A similar experiment in which SO_2 also was present only produced 7.6×10^{15} ions of surface nitrate species, which corresponds to a reduction by almost 40% ($[\text{NO}_2]=2.1 \times 10^{13}$ molecule cm^{-3} , $[\text{SO}_2]=2.4 \times 10^{12}$ molecule cm^{-3} and reaction time=150 min).

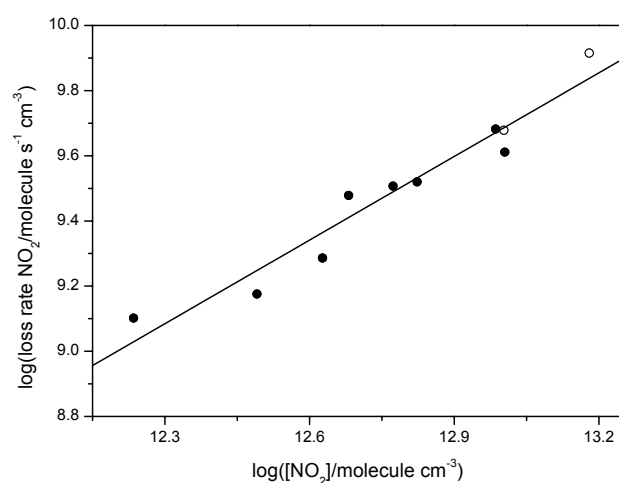


Fig. 7. Bilogarithmic plot of the loss rate of NO_2 as a function of $[\text{NO}_2]$. Filled circles are from experiments with both SO_2 and NO_2 present, open circles are from experiments with only NO_2 . The reaction order was determined to be $n=0.85\pm 0.28$ (2σ), $r^2=0.90$, from linear regression of the experiments with SO_2 and NO_2 present (filled circles).

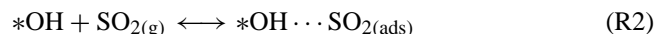
3.4 Mechanism

The reaction of NO_2 with surface adsorbed water is well-known and has been shown to be first order in NO_2 (Jenkin et al., 1988; Kleffmann et al., 1998; Langer et al., 1997; Mertes and Wahner, 1995; Pitts et al., 1984; Sakamaki, et al., 1983; Svensson et al., 1987).



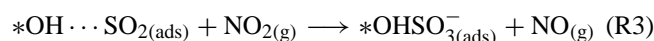
In this study the experiments were performed under “dry” conditions. However, some adsorbed water will be present in the dust sample, since the samples were only heated to 333 K prior to exposure. Different types of water-related reactive sites are present on the surface in the form of O^- or OH groups. The surface adsorbed water present during the experiment has not been quantified.

A previous study of the uptake of SO_2 proposed a two step mechanism for the oxidation of SO_2 where the first step is a reversible adsorption of SO_2 onto the surface followed by a second, irreversible reaction in which adsorbed SO_2 is oxidized to sulfate (Ullerstam et al., 2002).



were $*\text{OH}$ denotes free surface OH groups.

In the present investigation the oxidant is gaseous NO_2 which reacts with the surface adsorbed SO_2 forming surface sulfate and NO which escapes to the gas phase.



There would appear to be a competition for NO_2 , between surface adsorption forming nitrate, and its acting as an

oxidant, forming sulfate (i.e. reaction (R1) vs. (R3)). The oxidation is not fast enough to be the only process on the surface: the surface formation of nitrates is also taking place. This is also indicated by the reduction of surface nitrate products from the experiments in which both reactive gases are present compared, to experiments with only NO₂ exposure.

4 Discussion

The uptake coefficients for SO₂ in the presence of NO₂ measured using the two different techniques differ by a factor of around 10³ and 2×10⁴ (“geometric” and BET ratios, respectively), where the DRIFTS technique produces the lower results. This cannot be accounted for by the lower time resolution of the DRIFTS technique. The uptake coefficients obtained using the two techniques are fundamentally different. The Knudsen cell measures the loss rate of gaseous species during exposure, while the DRIFTS technique determines the rate of formation of products on the surface. In the Knudsen experiments there is no difference between the uptake coefficients measured using pure SO₂ or NO₂, and the uptake coefficient measured in experiments with both reactive gases present. The NO₂ has no effect on the measured “initial” uptake of SO₂ in these experiments. This is likely because the rate of physisorption is faster than the rate of sulfate formation and thus the uptake coefficient is determined by the rate of physisorption. However, the measured “reactive” uptake for SO₂ from the DRIFTS experiments is strongly affected by the presence of NO₂. In these experiments there would be no quantitative formation of sulfate on the surface without an oxidant present (in this case NO₂). It is implied that the initial uptake coefficient from the Knudsen experiments, in this case, is related to a reversible process and not with any reactive uptake. From the amount of adsorbed SO₂ in the Knudsen experiment and the measured formation rate of sulfate from the DRIFTS experiment we can make a rough estimate of a first order rate coefficient for the formation of sulfate on the surface. From Fig. 5 it can be estimated that a total amount of 5.9×10¹⁰ molecule cm⁻² has been adsorbed to the surface after 9 min. From a DRIFTS experiment, with [SO₂]=4.9×10¹² and [NO₂]=2.3×10¹³ (molecule cm⁻³), the rate of sulfate formation was determined to be 9.4×10⁶ ions s⁻¹ cm⁻². This would give an apparent first order rate coefficient of 1.6×10⁻⁴ s⁻¹ (depending on the NO₂ concentration) which leads to an estimated natural lifetime for the adsorbed SO₂ on the surface to be <2 hours.

There have been a number of studies concerning the uptake of NO₂ and SO₂ on different surfaces or materials. Very often substances that are components of crustal material are used, such as Al₂O₃, Fe₂O₃, MgO, and SiO₂. There are also a few studies in which natural dust samples have been used. One such study investigated the uptake of NO₂ and reported uptake coefficients of the order of 10⁻⁶ on China Loess and

Saharan sand (Underwood et al., 2001). An uptake coefficient for SO₂ on China Loess of the order of 10⁻⁵ has also been reported (Usher et al., 2002). This is a factor of ten higher than our result for both NO₂ and SO₂. The SO₂ deposition velocity on limestone and sandstone in the presence of NO₂ has been reported with a maximum of 0.45 cm s⁻¹ (Ausset et al., 1996). A rough estimate of the equivalent uptake coefficient from the deposition velocity can be made using the expression $\gamma=4 v_d/v_m$, where the v_d is the deposition velocity and v_m the molecular velocity (Dentener et al., 1996). The uptake coefficient is estimated to be 5×10⁻⁵, which is also around a factor of ten higher than our result.

The difference in uptake coefficient from our work compared to coefficients found in the literature is more likely due to a difference between substances than in experimental artefacts. For example the sample of Saharan sand used by Underwood et al. (2001), has a BET surface area of 31 cm² mg⁻¹ and a particle diameter of 250 μm compared to our mineral dust sample which has a BET surface area of 500 cm² mg⁻¹ and diameter of <20 μm. The China loess sample, which has a different composition than Saharan sand, used by Underwood et al. (2001) and Usher et al. (2002) has a BET surface area of 110 cm² mg⁻¹. It is expected that natural mineral samples with different compositions and characteristics will have different reactivities.

The uptake coefficients obtained using the BET surface area as the reactive surface area should be considered to be lower limits. The BET surface area of the dust is relatively large and the dust particle is expected to be quite porous (Ullerstam et al., 2002). This means that some parts may be less accessible to the reactive gas due to pore resistance and that the BET surface area may not be a relevant measure of the reactive surface.

The formation of surface sulfate is an important characteristic since it changes the physical properties of the mineral dust particle. A particle coated with sulfate is hygroscopic and will take up water; it may therefore take up more SO₂ into this aqueous layer that would otherwise be formed (Zhang and Chan, 2002). In a previous study on the same mineral dust sample it has been shown that the dust has a capacity to neutralize an acidified leaching solution (Desboeufs et al., 2003). It has also been shown in a previous study that the presence of water vapor regenerates the surface of the mineral dust and hence enhances the capacity of sulfate formation (Ullerstam et al., 2002). These observations, together with the fact that water vapour is always present in the atmosphere means that dust particles may alternate between being wet and dry. Since wet-dry cycling of the dust particles increases the sulfate forming capacity, it is likely that the mineral dust particles have a greater capacity for sulfate formation than suggested by the reactive uptake studies alone.

To be able to compare the lifetime and the importance of heterogeneous reactions with other losses such as gas phase reactions the heterogeneous rates were translated to a

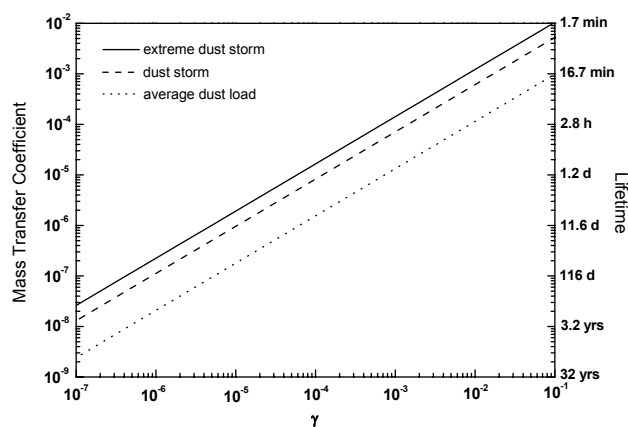


Fig. 8. Calculated mass transfer coefficients as a function of the heterogeneous uptake, γ , as described in the text Li et al. (2001). Data used for the calculations: Diffusion constant (D), $0.126 \text{ cm}^2 \text{ s}^{-1}$, Lognormal distribution for mineral dust: $N(\text{average})=798$, $N(\text{storm})=2800$, $N(\text{extreme storm})=5600$; r , $0.88 \mu\text{m}$; $\log(\sigma)$, 0.23 ; $\rho_s=2.0 \mu\text{g m}^{-3}$ (Li et al., 2001; Zhang et al., 1999; Alpert et al., 2001).

pseudo-first order mass transfer constant as described by Li and co-workers (Li et al., 2001).

$$k_j = \int_{r_2}^{r_1} 4\pi r^2 F(r) \frac{dn}{dr} dr \quad (10)$$

$$F(r) = \frac{D_j/r}{1 + f(K_n, \gamma)K_n} \quad (11)$$

$$f(K_n, \gamma) = \frac{1.333 + 0.71K_n^{-1}}{1 + K_n^{-1}} + \frac{4(1 - \gamma)}{3\gamma} \quad (12)$$

where k_j is the overall mass transfer coefficient, in $\text{cm}^3 \text{ s}^{-1}$, for species j ; D_j is the gas phase diffusion coefficient in $\text{cm}^2 \text{ s}^{-1}$; K_n is the dimensionless Knudsen number ($=\lambda/r$), λ is the effective free path of a gas molecule in air; r is the particle radius; $F(r)$ is the flux of the trace species to the surface of the aerosol particle with radius r in molecule cm s^{-1} ; dn/dr is the number-size distribution of aerosol particles, and γ is the uptake coefficient.

The mass transfer coefficient (k_j) was calculated from the above expressions as a function of uptake coefficient by using the lognormal distribution for the aerosol number-size distribution.

$$\frac{dn(r)}{d(\log r)} = \sum_{i=1}^3 \frac{N_i}{\log \sigma_i \sqrt{2\pi}} \exp \left\{ \frac{-(\log r/R_i)^2}{2(\log \sigma_i)^2} \right\} \quad (13)$$

where r is the particle radius in μm , $n(r)$ is the cumulative particle number distribution in cm^{-3} for particles larger than r , R is the mean particle radius in m, n is the integral of the lognormal function, and $\log \sigma$ is a measure of particle polydispersity.

The corresponding lifetime is calculated as a function of γ as is shown in Fig. 8. The lifetime of SO_2 calculated from the reaction with OH radicals in the gas phase is equal to 13 days ($k=8.8 \times 10^{-13} \text{ cm}^3 \text{ molecule}^{-1} \text{ s}^{-1}$ and $[\text{OH}]=1 \text{ times } 10^6 \text{ molecule cm}^{-3}$) (DeMore et al., 1997). From the plot it can be seen that this would correspond to a γ in the order of around 4×10^{-5} in the average dust load scenario. The lifetime of NO_2 in the gas phase is even lower considering the reaction with OH radicals and O_3 which corresponds to 16 h and 3.5 h respectively ($k_{\text{OH}}=8.8 \times 10^{-12}$ and $k_{\text{O}_3}=3.2 \times 10^{-17}$ in $\text{cm}^3 \text{ molecule}^{-1} \text{ s}^{-1}$, $[\text{OH}]=1 \times 10^6$ and $[\text{O}_3]=2.5 \times 10^{12}$ in molecule cm^{-3}).

Comparing this with the reactive uptake from the DRIFTS experiments it is apparent that the formation of sulfate on mineral dust by oxidation of NO_2 is not an important sink of gas phase SO_2 . Without the appropriate oxidant present the SO_2 trapped on the dust surface is more likely to be desorbed than oxidized to sulfate, as evident from the different values of uptake coefficient determined by the two different techniques. For example, with ozone as the oxidant the reactive uptake coefficient ($\gamma=5 \times 10^{-7}$) is large enough to be a competitive sink for SO_2 during episodes of high dust loading in the atmosphere (Ullerstam et al., 2002).

Acknowledgements. We would like to thank Thomas Rosenørn and Jacob Mønster for help with the Knudsen cell. This work was supported by the Nordic Network for Chemical Kinetics funded by the Nordic Academy for Advanced Study, and the Danish Natural Sciences Research Council.

References

- Ausset, P., Crovisier, J. L., del Monte, M., Furlan, V., Girardet, F., Hammecker, C., Jeannette, D., and Lefevre, R. A.: Experimental study of limestone and sandstone sulphation in polluted realistic conditions: The Lausanne Atmospheric Simulation Chamber (LASC), *Atmos. Environ.*, 30, 3197–3207, 1996.
- Borensen, C., Kirchner, U., Scheer, V., Vogt, R., and Zellner, R.: Mechanism and kinetics of the reactions of NO_2 or HNO_3 with alumina as a mineral dust model compound, *J. Phys. Chem. A*, 104, 5036–5045, 2000.
- Carmichael, G. R., Zhang, Y., Chen, L. L., Hong, M. S., and Ueda, H.: Seasonal variation of aerosol composition at Cheju Island, Korea, *Atmos. Environ.*, 30, 2407–2416, 1996.
- Chang, C. C.: Infrared Studies of SO_2 on Gamma-Alumina, *J. Catalysis*, 53, 374–385, 1978.
- Datta, A., Cavell, R. G., Tower, R. W., and George, Z. M.: Claus Catalysis I. Adsorption of SO_2 on the Alumina Catalyst studied by Ftir and Electron-Paramagnetic-Res Spectroscopy, *J. Phys. Chem.*, 89, 443–449, 1985.
- Dentener, F. J., Carmichael, G. R., Zhang, Y., Lelieveld, J., and Crutzen, P. J.: Role of mineral aerosol as a reactive surface in the global troposphere, *J. Geophys. Res.-A*, 101, 22 869–22 889, 1996.
- Deo, A. V. and Dalla Lana, I. G.: Infrared studies of the adsorption and surface reactions of hydrogen sulfide and sulfur dioxide on some aluminas and zeolites, *J. Catalysis*, 21, 270–281, 1971.

- Desboeufs, K. V., Losno, R., and Colin, J. L.: Relationship between droplet pH and aerosol dissolution kinetics: Effect of incorporated aerosol particles on droplet pH during cloud processing, *J. Atmos. Chem.*, 46, 159–172, 2003.
- Desboeufs, K. V., Losno, R., Vimeux, F., and Cholbi, S.: The pH-dependent dissolution of wind-transported Saharan dust, *J. Geophys. Res.-A*, 104, 21 287–21 299, 1999.
- Galy-Lacaux, C., Carmichael, G. R., Song, C. H., Lacaux, J. P., Al Ourabi, H., and Modi, A. I.: Heterogeneous processes involving nitrogenous compounds and Saharan dust inferred from measurements and model calculations, *J. Geophys. Res.-A*, 106, 12 559–12 578, 2001.
- Golden, D. M., Spokes, G. N., and Benson, S. W.: Very low-pressure pyrolysis (VLPP): A versatile kinetic tool, *Angewandte Chemie International Edition*, 12, 534–546, 1973.
- Goodman, A. L., Li, P., Usher, C. R., and Grassian, V. H.: Heterogeneous uptake of sulfur dioxide on aluminum and magnesium oxide particles, *J. Physical Chemistry A*, 105, 6109–6120, 2001.
- Grassian, V. H.: Chemical reactions of nitrogen oxides on the surface of oxide, carbonate, soot, and mineral dust particles: Implications for the chemical balance of the troposphere, *Journal of Physical Chemistry A*, 106, 860–877, 2002.
- Hadjiivanov, K., Bushev, V., Kantcheva, M., and Klissurski, D.: Infrared-Spectroscopy Study of the Species Arising During NO₂ Adsorption on TiO₂ (Anatase), *Langmuir*, 10, 464–471, 1994.
- Jenkin, M. E., Cox, R. A., and Williams, D. J.: Laboratory studies of the kinetics of formation of nitrous acid from the thermal reaction of nitrogen dioxide and water vapour, *Atmos. Environ.*, 22, 487–498, 1988.
- Kleffmann, J., Becker, K. H., and Wiesen, P.: Heterogeneous NO₂ conversion processes on acid surfaces: Possible atmospheric implications, *Atmos. Environ.*, 32, 2721–2729, 1998.
- Langer, S., Pemberton, R. S., and Finlayson-Pitts, B. J.: Diffuse reflectance infrared studies of the reaction of synthetic sea salt mixtures with NO₂: A key role for hydrates in the kinetics and mechanism, *J. Phys. Chem. A*, 101, 1277–1286, 1997.
- Li, P., Perreau, K. A., Covington, E., Song, C. H., Carmichael, G. R., and Grassian, V. H.: Heterogeneous reactions of volatile organic compounds on oxide particles of the most abundant crustal elements: Surface reactions of acetaldehyde, acetone, and propionaldehyde on SiO₂, Al₂O₃, Fe₂O₃, TiO₂, and CaO, *J. Geophys. Res.-A*, 106, 5517–5529, 2001.
- Martin, R. V., Jacob, D. J., Yantosca, R. M., Chin, M., and Ginoux, P.: Global and regional decreases in tropospheric oxidants from photochemical effects of aerosols, *J. Geophys. Res.-A*, 108, 4097–4115, 2003.
- Mertes, S. and Wahner, A.: Uptake of Nitrogen-Dioxide and Nitrous-Acid on Aqueous Surfaces, *J. Phys. Chem.*, 99, 14 000–14 006, 1995.
- Meyer, B., Ospina, M., and Peter, L. B.: Raman Spectrometric Determination of Oxysulfur Anions in Aqueous Systems, *Analytica Chimica Acta*, 117, 301–311, 1980.
- Mønster, J., Rosenørn, T., Nielsen, O. J., and Johnson, M. S.: Knudsen cell construction, validation and studies of the uptake of oxygenated fuel additives on soot, *Environ. Science & Pollution Res., Special Issue 1*, 63–67, 2002.
- Nakamoto, K.: *Infrared and Raman Spectra of Inorganic and Coordination Compounds*, Wiley & Sons, New York, 1997.
- Nishikawa, M., Kanamori, S., Kanamori, N., and Mizoguchi, T.: Kosa Aerosol as Eolian Carrier of Anthropogenic Material, *Sci. Total Environ.*, 107, 13–27, 1991.
- Pitts, J. N. J., Sanhueza, E., Atkinson, R., Carter, W. P. L., Winer, A. M., Harris, G. W., and Plum, C. N.: An investigation of the dark formation of nitrous acid in environmental chambers, *Int. J. Chem. Kinetics*, 16, 919–939, 1984.
- Rognon, P., Coude-Gaussen, G., Revel, M., Grousset, F. E., and Pedemay, P.: Holocene Saharan dust deposition on the Cape Verde islands: Sedimentological and Nd-Sr isotopic evidence, *Sedimentology*, 43, 359–366, 1996.
- Sakamaki, F., Hatakeyama, S., and Akimoto, H.: Formation of nitrous acid and nitric oxide in the heterogeneous dark reaction of nitrogen dioxide and water vapour in a smog chamber, *Int. J. Chem. Kinetics*, 15, 1013–1029, 1983.
- Schoonheydt, R. A. and Lunsford, J. H.: Infrared Spectroscopic Investigation of the Adsorption and Reactions of SO₂ and MgO, *J. Catalysis*, 26, 261–271, 1972.
- Svensson, R., Ljungstrom, E., and Lindqvist, O.: Kinetics of the Reaction between Nitrogen-Dioxide and Water-Vapor, *Atmos. Environ.*, 21, 1529–1539, 1987.
- Tabor, K., Gutzwiller, L., and Rossi, M. J.: Heterogeneous Chemical-Kinetics of NO₂ on Amorphous-Carbon at Ambient-Temperature, *J. Phys. Chem.*, 98, 6172–6186, 1994.
- Tegen, I. and Fung, I.: Modeling of Mineral Dust in the Atmosphere - Sources, Transport, and Optical-Thickness, *J. Geophys. Res.-A*, 99, 22 897–22 914, 1994.
- Tsyganenko, A. A. and Mardilovich, P. P.: Structure of alumina surfaces, *J. Chemical Society-Faraday Transactions*, 92, 4843–4852, 1996.
- Ullerstam, M., Vogt, R., Langer, S., and Ljungstrom, E.: The kinetics and mechanism of SO₂ oxidation by O₃ on mineral dust, *Phys. Chem. Chem. Phys.*, 4, 4694–4699, 2002.
- Underwood, G. M., Li, P., Usher, C. R., and Grassian, V. H.: Determining accurate kinetic parameters of potentially important heterogeneous atmospheric reactions on solid particle surfaces with a Knudsen cell reactor, *J. Phys. Chem. A*, 104, 819–829, 2000.
- Underwood, G. M., Miller, T. M., and Grassian, V. H.: Transmission FT-IR and Knudsen cell study of the heterogeneous reactivity of gaseous nitrogen dioxide on mineral oxide particles, *J. Phys. Chem. A*, 103, 6184–6190, 1999.
- Underwood, G. M., Song, C. H., Phadnis, M., Carmichael, G. R., and Grassian, V. H.: Heterogeneous reactions of NO₂ and HNO₃ on oxides and mineral dust: A combined laboratory and modeling study, *J. Geophys. Res.-A*, 106, 18 055–18 066, 2001.
- Usher, C. R., Al-Hosney, H., Carlos-Cuellar, S., and Grassian, V. H.: A laboratory study of the heterogeneous uptake and oxidation of sulfur dioxide on mineral dust particles, *J. Geophys. Res.-A*, 107, 4713, doi:10.1029/2002JD002051, 2002.
- Zhang, D. Z., Shi, G. Y., Iwasaka, Y., and Hu, M.: Mixture of sulfate and nitrate in coastal atmospheric aerosols: individual particle studies in Qingdao (36 degrees 04' N, 120 degrees 21' E), China, *Atmos. Environ.*, 34, 2669–2679, 2000.
- Zhang, Y. and Carmichael, G. R.: The role of mineral aerosol in tropospheric chemistry in East Asia – A model study, *J. App. Meteor.*, 38, 353–366, 1999.
- Zhang, Y. H. and Chan, C. K.: Understanding the hygroscopic properties of supersaturated droplets of metal and ammonium sulfate solutions using raman spectroscopy, *J. Phys. Chem. A*, 106, 285–292, 2002.